J Solid State Electrochem (2012) 16:265–271
DOI 10.1007/s10008-011-1316-9

ORIGINAL PAPER

Improvement of overcharge performance using $Li_4Ti_5O_{12}$ as negative electrode for $LiFePO_4$ power battery

Wei Cui · Yan-Bing He · Zhi-Yuan Tang · Quan-Hong Yang · Qiang Xu · Fang-Yuan Su · Li Ma

Received: 30 November 2010 / Revised: 10 January 2011 / Accepted: 14 January 2011 / Published online: 8 February 2011

Abstract Liquid state soft packed $LiFePO_4$ cathode lithium ion cells with capacity of 2 Ah were fabricated using graphite or $Li_4Ti_5O_{12}$ as negative electrodes to investigate the 3 C/10 V overcharge characteristics at room temperature. The $LiFePO_4/Li_4Ti_5O_{12}$ cell remained safe after the 3 C/10 V overcharge test while the $LiFePO_4$/graphite cell went to thermal runaway. Temperature and voltage variations during overcharge were recorded and analyzed. The cells after overcharge were disassembled to check the changes of the separated cell components. The results showed that the $Li_4Ti_5O_{12}$ as anode active material for $LiFePO_4$ cell showed obvious safety advantage compared with the graphite anode. The lithium ionic diffusion models of $Li_4Ti_5O_{12}$ anode and graphite anode were built respectively with the help of morphology characterizations performed by scanning electron microscopy. It was found that the different particle shapes and lithium ionic diffusion modes caused different lithium ionic conductivities during overcharge process.

W. Cui · Z.-Y. Tang · Q.-H. Yang · Q. Xu · F.-Y. Su
Department of Applied Chemistry, School of Chemical Engineering and Technology, Tianjin University, Tianjin 300072, China

W. Cui
e-mail: tju_cuiwei@126.com

Y.-B. He (✉)
Advanced Materials Institute, Graduate School at Shenzhen, Tsinghua University, Shenzhen 518055, China
e-mail: hezuzhang_2000@163.com

L. Ma
McNair Technology Co., Ltd, Dongguan, Guangdong 523700, China

Keywords Overcharge performance · Safety · $Li_4Ti_5O_{12}$ · Graphite · $LiFePO_4$

Introduction

The demand for safer batteries has created a dynamic research interest in improving the currently available lithium battery systems. $LiFePO_4/Li_4Ti_5O_{12}$ battery system is promising as an electric vehicle battery system for its excellent power and safety performance. Lithium iron phosphate ($LiFePO_4$) cathode active material is excellent in terms of safety, cycle life, and cost [1]. These unique properties make the $LiFePO_4$ positive electrode batteries play a prominent role as ideal electrochemical storage systems in renewable energy utilization as well as power systems for sustainable vehicles. However, the lithium ion batteries for these applications are still problematic, especially the safety issues that are still to be resolved. Many safety issues happen due to thermal runaway, which is attributed to self-acceleration leading to the increase of the battery temperature at unsuitable voltage charging. The lithiated negative electrode and de-lithiated positive electrode materials are very reactive during overcharge. Compared with the $LiCoO_2$, the $LiFePO_4$ is much more stable at de-lithiated state [2].

However, the anode is considered to be more important for safety issues because the full-charged state is much more unstable than the full-discharged state of lithium ion cells, and the lithium ions are enriched at full-charged anode where the lithium dendrite is highly prone to form. Therefore, many researches focus on the sticking point of safety issues on negative electrode materials for $LiFePO_4$ batteries [3–7]. At present, the most widely used negative electrode material is graphite [3]. The full-charged graphite

anode can react with the electrolyte components easily under abusive conditions, whereas there has been considerable interest in $Li_4Ti_5O_{12}$ as a potential anode active material for use in lithium ion batteries [7]. It possesses many advantages compared to the currently used graphite anode, especially as a zero-strain lithium insertion host suggesting virtually unlimited cycle life [8]. In addition, graphite has distinct crystal expansion at charged state [9], which would enhance the instability of the electrode.

$Li_4Ti_5O_{12}$ features a flat operating voltage of about 1.55 V versus lithium metal, which is above the reduction potential of the common electrolyte solvents. Thus, the solid electrolyte interface cannot be formed on the surface of the $Li_4Ti_5O_{12}$ anode, which should be a favorable property for high rate operation [10]. Although the electronic conductivity of the $Li_4Ti_5O_{12}$ is lower three orders of magnitude than that of the graphite [11], the higher lithium ionic conductivity makes the $Li_4Ti_5O_{12}$ safer for high rate operation [12].

There are some reports about the electrochemical performance of $LiFePO_4/Li_4Ti_5O_{12}$ battery system [4, 13] and investigations of the overcharge performance of the $LiCoO_2$/graphite system [14–17], whereas the characterizations about the safety performance of $LiFePO_4/Li_4Ti_5O_{12}$ battery system is seldom till now, especially the reports about the overcharge performance. The overcharge performance is considered as the most important safety test due to much additional energy added to the cell during overcharge [14].

In this work, we investigated the overcharge behavior of $LiFePO_4/Li_4Ti_5O_{12}$ cell and compared with that of the $LiFePO_4$/graphite cell. It was found that the $LiFePO_4/Li_4Ti_5O_{12}$ system showed more excellent overcharge performance than that of the $LiFePO_4$/graphite system. The reasons for the thermal behaviors and the models of the lithium ionic diffusion of different anodes during overcharge were analyzed.

Experimental

0440130-type liquid state soft packed lithium ion cells, which are nominally 4 mm thick, 40 mm wide, and 130 mm long, were assembled. The cathode constituents were $LiFePO_4$ (ALEES, Taiwan), Super P black (Mitsubishi, Japan), and polyvinylidene fluoride (PVDF) coated over an aluminum current collector in the weight ratio of 85%, 10%, and 5%, respectively. The anode material constituents were coated over a copper current collector and comprised a blend made up of graphite (BTR, China), Super P black (Mitsubishi, Japan), and PVDF in a weight ratio of 90%, 7%, and 3%, or a blend made up of $Li_4Ti_5O_{12}$ (Tianjiao, China), Super P black (Mitsubishi), and PVDF in a weight ratio of 90%, 7%, and 3%, respectively. Many battery manufacturers apply deionized water and SBR (styrene butadiene rubber) to be the anode solvent and binder for graphite anode. For the coherence of this test, NMP as the solvent and PVDF as the binder were applied to the fabrication of the two kinds of anodes.

The electrolyte (Tinci, China) was 1 M $LiPF_6$ in EC (ethyl carbonate)/DMC (dimethyl carbonate) (1:1, v/v) solution without any other additives, such as safety protection agents or fire retardant additives. The separator was microporous PE (polyethylene) membrane (UBE, Japan).

The anodes, cathodes, and separators were rolled together to form the cell cores and then the cores were set into aluminum–plastic film boxes used as soft packs. The electrolyte was thereafter injected and the cells were sealed with a sealing machine. After formation, the formation gas was removed with a vacuum degassing machine, and then the airbags were cut and the remained edges were sealed to form the 0440130-type cells. There were no protective circuits fixed on the cells.

Morphology characterizations were performed by scanning electron microscopy (SEM; Philips FEI SIKION FESEM, Netherlands) utilized to characterize the initial state of the electrodes. Charge–discharge characteristics were performed on a cell cycle test system (RePower, China). Cycle performance of the $LiFePO_4/Li_4Ti_5O_{12}$ cells was evaluated at different rates between 1.2 V and 2.4 V, and the $LiFePO_4$/graphite cells from 2.7 V to 3.7 V. All the cells were charged at room temperature by the constant-current/constant-voltage (CC–CV) protocol. That is, the cells were charged at a certain current rate until the voltage reached to a limited voltage, followed by holding the voltage until the current dropped to 50 mA.

The initial SOC (state of charge) of all the cells before overcharge was 0%. The overcharge tests of cells were carried out at a constant current of 6 A (3 C) and an impressed voltage of 10 V by means of a direct current charger (GVE, China). During the overcharge tests, the cell temperature variations as a function of time were recorded by means of an electronic digital thermometer (TES, Taiwan) with a thermocouple probe fixed tightly over the surface of the cells. The voltage and current variations with time were illustrated on the direct current charger and recorded artificially every 5 s. A designed and locally fabricated protecting iron box was used for preventing explosive splash injury. The operation terminated when the cell current was less than 50 mA. After the tests, each overcharged cell was carefully disassembled and the surface characteristics of cathode, anode, and separator were analyzed separately in an argon-filled glove box.

Results and discussion

Figure 1 shows the discharge profiles of the $LiFePO_4$/$Li_4Ti_5O_{12}$ and $LiFePO_4$/graphite cells at 1 C, 3 C, and 6 C, respectively. It can be found that the discharge voltage plateaus of the cells decreases at the higher rates (3 C or 6 C) compared with those at the low discharge rate (1 C) due to polarization. The $LiFePO_4$/$Li_4Ti_5O_{12}$ cell presents excellent discharge plateaus at different rates, while the $LiFePO_4$/graphite cell presents sloping discharge plateaus at different rates. Moreover, the discharge curves decreases rapidly at the end of the discharge plateaus of $LiFePO_4$/$Li_4Ti_5O_{12}$ cell, while that of $LiFePO_4$/graphite cell decreases smoothly. This is attributed to the de-lithiation characteristics of $Li_4Ti_5O_{12}$ and graphite anodes.

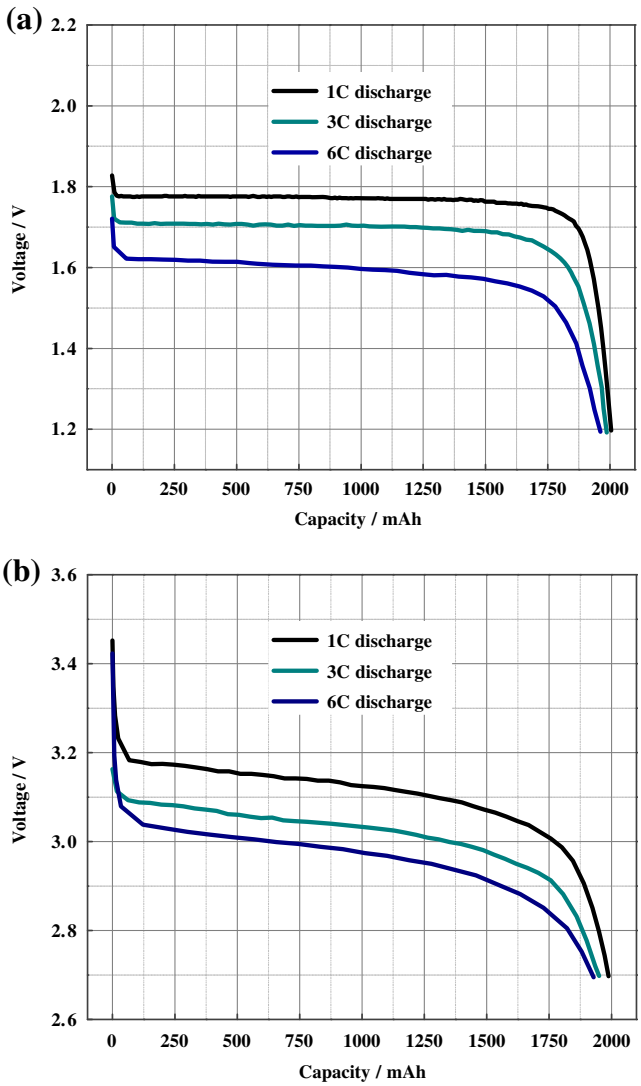

Fig. 1 Discharge profiles of two kinds of cells at different rates. **a** $LiFePO_4$/$Li_4Ti_5O_{12}$ cell. **b** $LiFePO_4$/graphite cell

It can also be obtained that the discharge capacity of $LiFePO_4$/$Li_4Ti_5O_{12}$ cell at discharge rate of 1 C, 3 C, and 6 C is 2,001.9 mAh, 1,983.6 mAh, and 1,943.4 mAh, respectively. The discharge capacity at rates of 3 C and 6 C is respective 99.09% and 97.78% of that at a rate of 1 C. These results show that the $LiFePO_4$/$Li_4Ti_5O_{12}$ cell can be discharged at a wide range of currents to deliver most of their capacity, indicating good rate discharge performance. For the $LiFePO_4$/graphite cell, the discharge capacity at discharge rate of 1 C, 3 C, and 6 C is 1,987.5 mAh, 1,950.5 mAh, and 1,928.1 mAh, respectively. The discharge capacity at rates of 3 C and 6 C is respectively 98.14% and 97.01% of that at a rate of 1 C. It is seen that the $LiFePO_4$/graphite cell also shows good high rate discharge performance.

Figure 2 presents the cycle performances of the two kinds of cells with a discharge rate of 1 C, 3 C, and 6 C. It can be found that the capacity retention of $LiFePO_4$/$Li_4Ti_5O_{12}$ cell after 100 cycles is 99.06% at discharge rate of 1 C, 96.38% at 3 C, and 96.01% at 6 C, respectively. For the $LiFePO_4$/graphite cells, the capacity retention after 100 cycles at a discharge rate of 1 C, 3 C, and 6 C is 98.81%, 98.50%, and 96.69%, respectively. Thus, the $LiFePO_4$/$Li_4Ti_5O_{12}$ and $LiFePO_4$/graphite cells all show excellent rate cycling performance.

Figure 3 exhibits the comparisons of the charge capacities of the CC and CV proportions. The two kinds of cells were charged at 0.1 C, 0.3 C, 0.5 C, 1 C, 2 C, 3 C, and 6 C, respectively, till the cells reached the fixed voltages ($LiFePO_4$/$Li_4Ti_5O_{12}$ cell at 2.4 V, $LiFePO_4$/graphite cell at 3.7 V), and then were charged at the fixed voltages till the current reducing to 50 mA. The CC

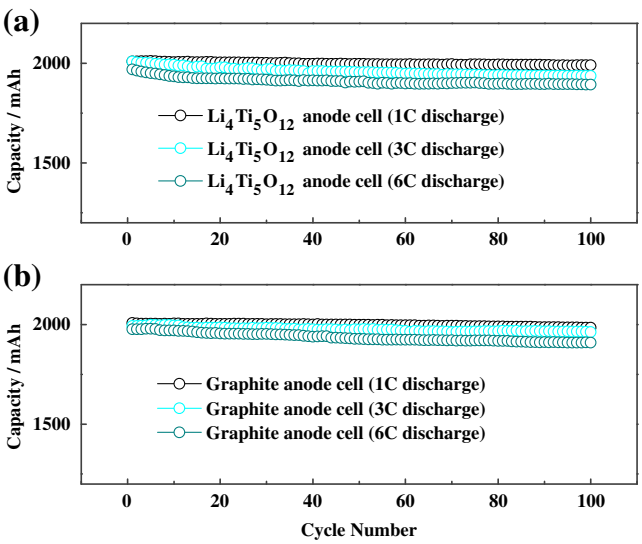

Fig. 2 Cycle performances of two kinds of cells at different rates. **a** $LiFePO_4$/$Li_4Ti_5O_{12}$ cell. **b** $LiFePO_4$/graphite cell

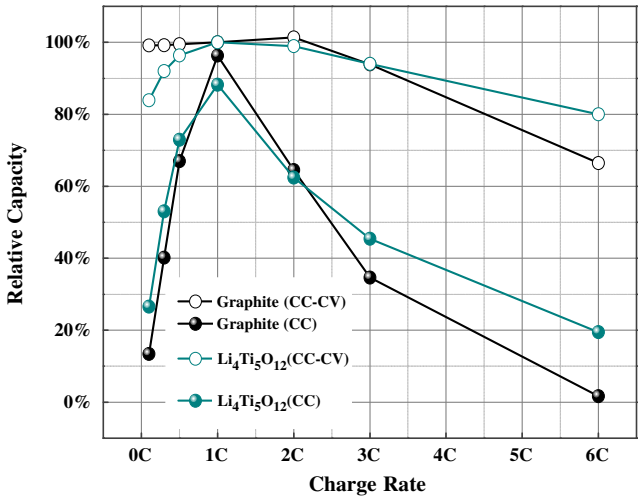

Fig. 3 Charge capacity ratios by CC and CV charge protocol

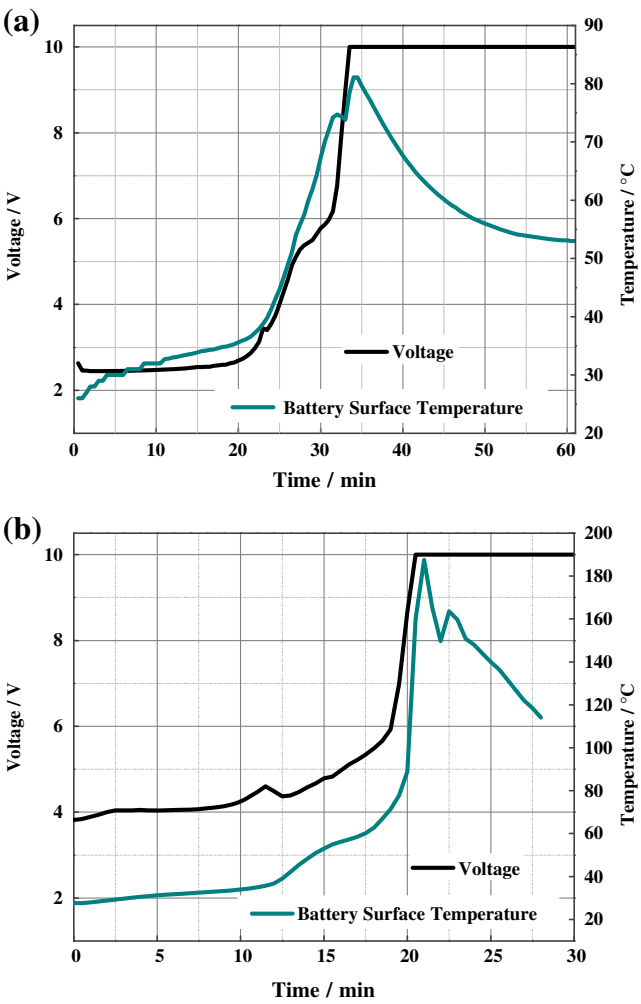

Fig. 4 Temperature and voltage variations of the cells during 3 C/10 V test. **a** $LiFePO_4/Li_4Ti_5O_{12}$ cell. **b** $LiFePO_4$/graphite cell

charging proportion decreases obviously when the charging rates are greater than 1 C for both types of cells. The CC charging proportion of $LiFePO_4/Li_4Ti_5O_{12}$ cell at 1 C is less than that of $LiFePO_4$/graphite cell due to the lower electronic conductivity of $Li_4Ti_5O_{12}$. But the CC charge proportion is greater than that of the $LiFePO_4$/graphite cell when the charging rates are greater than 1 C. This indicates the advantage of the $Li_4Ti_5O_{12}$ anode at high rate charge.

Figure 4 shows the temperature and voltage variation curves of the cells during 3 C/10 V overcharge tests. It can be seen from Fig. 4a that the charge plateau of the $Li_4Ti_5O_{12}$ anode cell is 2.4 V under 3 C/10 V overcharge protocol, which appears to be 0.5 V higher than the normal charge plateau of 1.9 V. It might be attributed to the polarization under high impressed voltage. The cell voltage increases from 2.4 V to 3.4 V and the temperature rises from 25 °C to 37 °C during the initial 24 min. This indicates that there are no abnormal reactions inside the cells and the temperature increase is due to the Joule heat under high current. Then the voltage slightly reduces and the temperature increases rapidly, which indicates the exothermal reaction of the electrolyte [17]. The cell surface temperature is below 81 °C. Apparently, although $Li_4Ti_5O_{12}$ anode cell expanded during the test, there was no electrolyte leakage, package cauterization, or breach, for the inner pressure is less than the rupture limit of the aluminum–plastic package. The $LiFePO_4/Li_4Ti_5O_{12}$ cell exhibits excellent overcharge performance.

For the $LiFePO_4$/graphite system, the temperature and voltage increase obviously after the cell is being charged for 12 min, which indicates that there is an exothermal reaction inside the cell. Compared with the $LiFePO_4/Li_4Ti_5O_{12}$ cell, it can be found by the plateau durations that the $LiFePO_4$/graphite cell cannot be fully charged while the $LiFePO_4/Li_4Ti_5O_{12}$ cell can be fully charged before the ends of the charge plateaus. In addition, the charge plateau of $LiFePO_4$/graphite cell under 3 C/10 V is 0.7 V higher than the normal charge plateau. The polarization of $LiFePO_4$/graphite cell under high impressed voltage is much higher than that of the $LiFePO_4/Li_4Ti_5O_{12}$ cell. After about 18 min, the temperature and voltage of the $LiFePO_4$/graphite cell abruptly increase, and the cell finally explodes. The temperature summit is 190 °C. Therefore, the overcharge performance of the $LiFePO_4$/graphite cell is obviously worse than that of the $LiFePO_4/Li_4Ti_5O_{12}$ cell.

For the $LiFePO_4$ cathode material, the strong covalent P–O bonds in the tetrahedral PO_4^{3-} anion are believed to inhibit oxygen loss. Heterosite $FePO_4$ is stable in air up to 600 °C, above which it transforms into quartz-like $FePO_4$

without losing oxygen [18]. The charged $LiFePO_4$ has a high onset temperature of 250 °C and exotherm peaks at 280 °C and 315 °C on the DSC profile [19]. According to the temperature curves in Fig. 4, both temperature summits are below 190 °C. Thus, at elevated temperature, $LiFePO_4$ is not the main factor for the explosion of the lithium ion cell at overcharge, as the heat generation mainly released from cathode is far away from the onset point of full cell thermal runaway. In addition, all the other components of the two cells are the same except the anodes, thus the graphite anode is the key factor to the thermal runaway.

It is seen from Fig. 5a that there is no rupture of the $Li_4Ti_5O_{12}$ anode after overcharge. However, the graphite anode is totally devastated for overcharge. The remaining explosion products of the graphite anode appear to be dehiscence and agglomeration. The spherical fusions sticking to the anode surface is LiOH [16], which is the degradation of lithium dendrite. The poignant overcharge process and ruined anode reveals the poorer overcharge endurance of the graphite anode than that of the $Li_4Ti_5O_{12}$ anode.

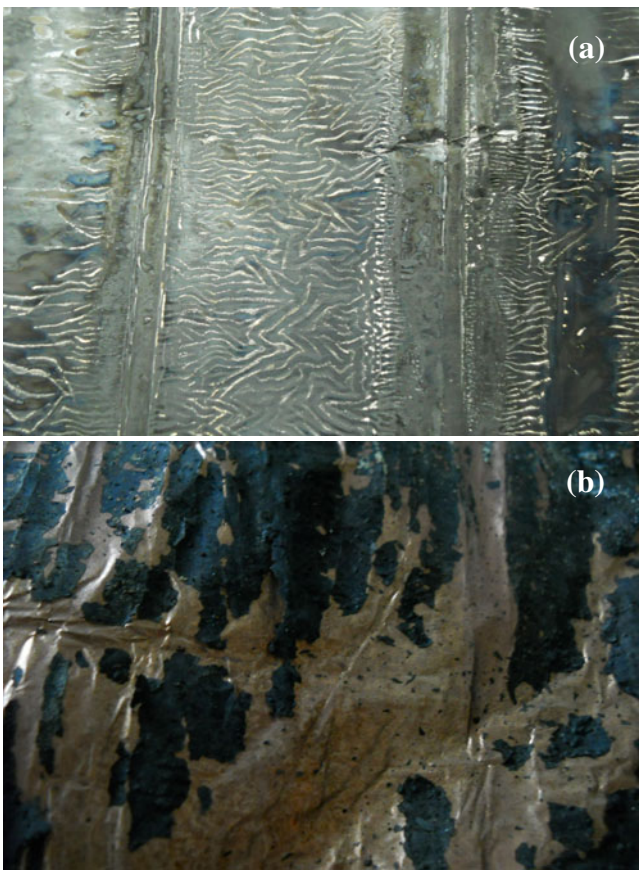

Fig. 5 Anodes after overcharge. **a** $Li_4Ti_5O_{12}$ anode surface. **b** Graphite anode surface

The two kinds of cells are different just for the anodes. So the different overcharge results are presumably due to the following reasons:

First reason is the SEI formation on the graphite surface. (1) The SEI formed in prismatic (edge) areas is enriched with inorganic compounds, while that in basal planes is enriched with organic compounds [20]. The uneven distribution of the SEI components causes uneven lithium ionic distribution which enhances the probability of lithium dendrite formation. (2) During charge process, lithium ions are intercalated into the graphite anode with a 10% crystal expansion of graphite along C-axis from de-lithiated state [9]. The expansion is more severe when the battery is overcharged, which influences the stability of the SEI. The overcharge even causes the destruction of the SEI, which makes the direct contact between the electrolyte and the electrode materials, and then initiating active material degradation [21]. (3) Heat from the SEI breakdown is considered as a trigger for thermal runaway during overcharge condition [22]. However, there is no SEI formed on the $Li_4Ti_5O_{12}$ material surface during charge process, avoiding the disadvantages mentioned above.

Second reason is the different lithium ionic conductivities of $Li_4Ti_5O_{12}$ and graphite. The ionic diffusion velocity of $Li_4Ti_5O_{12}$ is more than one order of magnitude higher than that of carbonaceous negative electrodes [23]. The lithium diffusion velocity is depending on the intrinsic crystal characteristics and the ionic diffusion pathways outside crystal particles. So the morphology difference is an important factor for the diffusion velocity. Figure 6 represents the graphite layers paralleling to the current collector inhibiting the ionic conductivity, which is attributed to the limitation of industrial slurry coating technique. This kind of morphology decelerates the lithium ionic diffusion of graphite anode. Higher quantity of lithium ions migrated from electrolyte under high current density increases the possibility of the formation of lithium dendrite due to the lower lithium ionic diffusion of the anode, which is an important factor to the thermal runaway [24–28], whereas the spinel structure of $Li_4Ti_5O_{12}$ determines the all-direction ionic pathway and the uniform particle sizes. The morphology of $Li_4Ti_5O_{12}$ anode surface as shown in Fig. 7 contributes to the lithium ion dispersion.

Several methods are applied industrially to solve the graphite-foil-parallel problem. (1) Magnetic force around the roasting oven to make the graphite vertical to current collector which was modeled in Fig. 8. (2) Ball milling to smooth the graphite edges and form spherical shape graphite particles. However, these methods cannot essentially change the ionic diffusion velocity of the carbona-

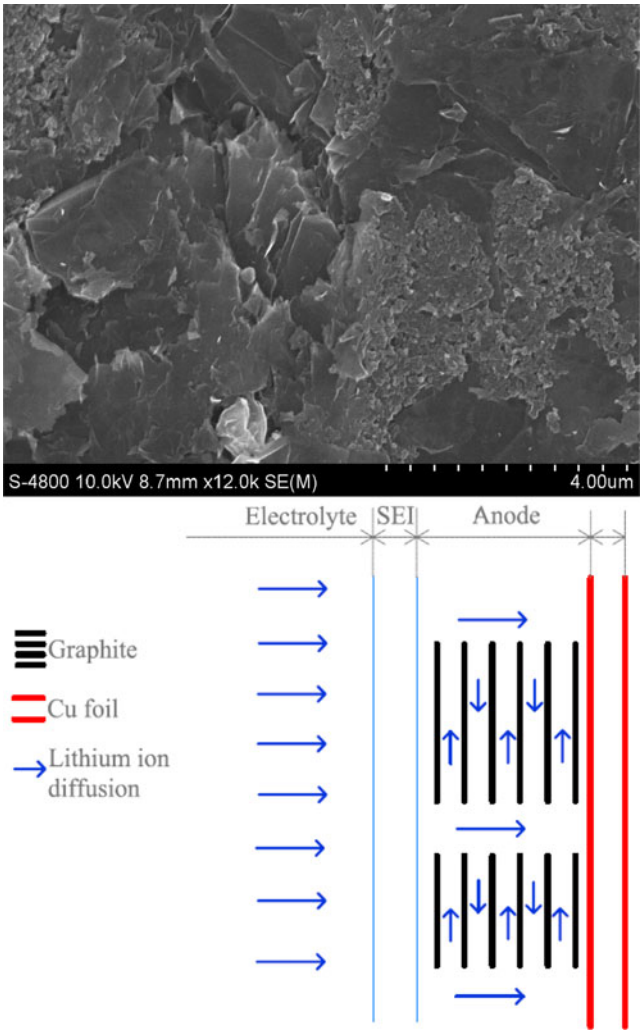

Fig. 6 Graphite layers parallel to current collector inhibiting the ionic diffusion

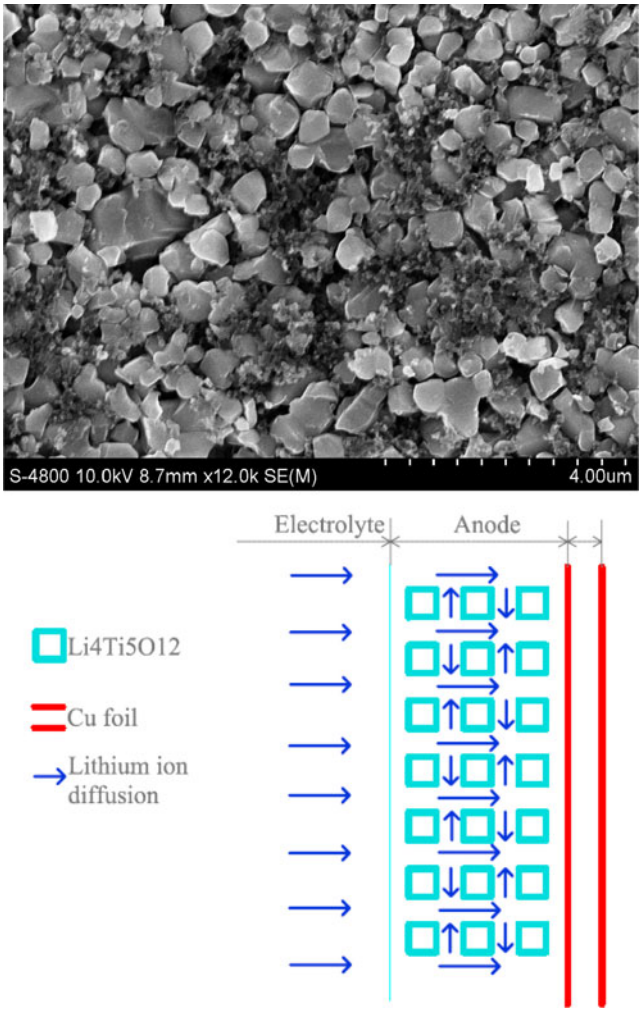

Fig. 7 Isotropic lithium ionic diffusion of $Li_4Ti_5O_{12}$ anode

ceous materials. In addition, it is supposed that all the graphite layers are vertical to the current collector; the graphite will face the electrolyte with its prismatic (edge) areas. Then the crystal expansion along the C-axis during charge process will be enlarged and the graphite particles are prone to desquamate from the current collector [9].

Conclusions

The 3 C/10 V protocol was applied to figure out the differences between $LiFePO_4/Li_4Ti_5O_{12}$ cell and $LiFePO_4$/graphite cell during overcharge. The cell with the $Li_4Ti_5O_{12}$ anode passed the overcharge test while the cell with the graphite anode went to thermal runaway. The infinitesimal crystal distortion and higher lithium ionic conductivity of $Li_4Ti_5O_{12}$ effectively prevent the cell from thermal runaway. However, the less lithium ionic conductivity, the SEI

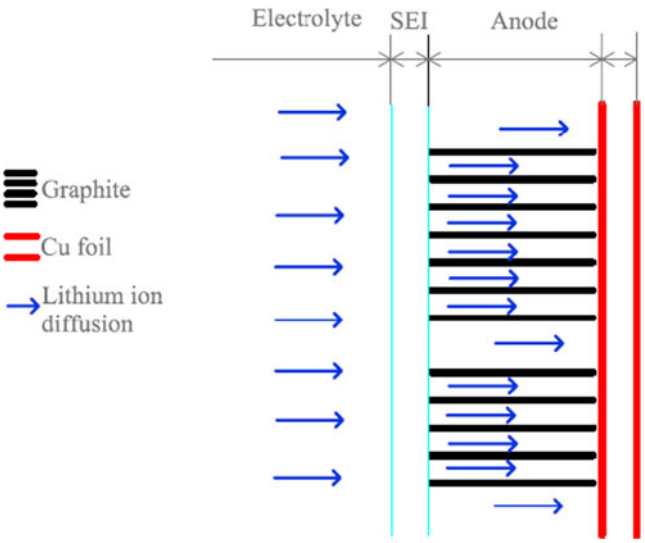

Fig. 8 Graphite prismatic areas facing electrolyte

instability, and the manufacture limitation of the graphite anode result in lesser stabilization of the graphite anode cell at overcharge.

Acknowledgment This work was supported by China Postdoctoral Science Foundation (No. 20100470296).

References

1. Roscher Ma, Vetter J, Sauer Du (2010) J Power Sources 195:3922–3927
2. Li G, Yang Z, Yang W (2008) J Power Sources 183:741–748
3. Abe T (2009) Secondary batteries—lithium rechargeable systems—lithium-ion | negative electrodes: carbon. Elsevier, Amsterdam
4. Scrosati B, Garche J (2010) J Power Sources 195:2419–2430
5. Yang J, Wang JL (2009) Secondary batteries—lithium rechargeable systems—lithium-ion | negative electrodes: lithium alloys. Elsevier, Amsterdam
6. Yamaki J (2009) Secondary batteries—lithium rechargeable systems—lithium-ion | overview. Elsevier, Amsterdam
7. Noguchi H (2009) Secondary batteries—lithium rechargeable systems—lithium-ion | negative electrode: titanium-based materials. Elsevier, Amsterdam
8. Kataoka K, Takahashi Y, Kijima N, Hayakawa H, Akimoto J, Ohshima K-I (2009) Solid State Ionics 180:631–635
9. Inaba M (2009) Secondary batteries—lithium rechargeable systems—lithium-ion | negative electrodes: graphite. Elsevier, Amsterdam
10. Wolfenstine J, Allen Jl (2008) J Power Sources 180:582–585
11. Takami N, Inagaki H, Kishi T, Harada Y, Fujita Y, Hoshina K (2009) J Electrochem Soc 156:A128–A132
12. Wolfenstine J, Lee U, Allen Jl (2006) J Power Sources 154:287–289
13. Morales J, Trócoli R, Franger S, Santos-Peña J (2010) Electrochim Acta 55:3075–3082
14. Spotnitz R, Franklin J (2003) J Power Sources 113:81–100
15. Tobishima S-I, Takei K, Sakurai Y, Yamaki J-I (2000) J Power Sources 90:188–195
16. Zeng Y, Wu K, Wang D, Wang Z, Chen L (2006) J Power Sources 160:1302–1307
17. Ohsaki T, Kishi T, Kuboki T, Takami N, Shimura N, Sato Y, Sekino M, Satoh A (2005) J Power Sources 146:97–100
18. Muñoz-Rojas D, Leriche J-B, Delacourt C, Poizot P, Palacín Mr, Tarascon J-M (2007) Electrochem Commun 9:708–712
19. Chen G, Richardson Tj (2010) J Power Sources 195:1221–1224
20. Peled E, Bar Tow D, Merson A, Gladkich A, Burstein L, Golodnitsky D (2001) J Power Sources 97–98:52–57
21. Veluchamy A, Doh C-H, Kim D-H, Lee J-H, Shin H-M, Jin B-S, Kim H-S, Moon S-I (2009) J Power Sources 189:855–858
22. Belov D, Yang M-H (2008) Solid State Ionics 179:1816–1821
23. Zaghib K, Simoneau M, Armand M, Gauthier M (1999) J Power Sources 81–82:300–305
24. Teyssot A, Rosso M, Bouchet R, Lascaud S (2006) Solid State Ionics 177:141–143
25. Rosso M, Brissot C, Teyssot A, Dollé M, Sannier L, Tarascon J-M, Bouchet R, Lascaud S (2006) Electrochim Acta 51:5334–5340
26. Harris Sj, Timmons A, Baker Dr, Monroe C (2010) Chem Phys Lett 485:265–274
27. Gerald Re, Klingler Rj, Sandí G, Johnson Cs, Scanlon Lg, Rathke Jw (2000) J Power Sources 89:237–243
28. Janot R, Guérard D (2005) Prog Mater Sci 50:1–92